Adaptive finite-time integral super-twisting sliding mode trajectory tracking control for unmanned surface vehicles under time-varying disturbances

Pham Van Thao[1] **and Hoang Duc Long**[2,*]

[1,2]*Le Quy Don Technical University*
[*]*Corresponding author E-mail: longhd@lqdtu.edu.vn*
DOI: https://doi.org/10.64032/mca.v30i4.431

Abstract

This article proposes a robust finite-time trajectory tracking controller for an unmanned surface vehicle operating in nonlinear marine environments affected by dynamic uncertainties and time-varying external disturbances. Unlike data-driven optimal learning approaches, the proposed method is fully model-based and emphasizes guaranteed transient performance under bounded but unknown disturbance levels. A new integral sliding variable is constructed to improve steady-state accuracy and reduce bias caused by persistent disturbances. A second-order super-twisting sliding mode mechanism is then incorporated to enhance robustness while alleviating the chattering commonly observed in conventional first-order sliding mode controllers. To avoid conservative gain selection, an online adaptive mechanism is developed to adjust the switching gains according to the instantaneous sliding-variable magnitude. A rigorous stability analysis is provided for the disturbed three-degree-of-freedom vehicle model, proving finite-time convergence of the sliding variable and asymptotic convergence of the tracking errors on the sliding manifold, with boundedness of all closed-loop signals. Simulation studies are conducted for a benchmark unmanned surface vehicle subject to wind-wave-current-type disturbances. The proposed controller is compared with a conventional sliding mode controller, a computed-torque proportional-derivative controller, and a backstepping-proxy controller. Quantitative indices, including RMSE, NICS, chattering index, and settling time, are reported to support the graphical results. The results demonstrate improved disturbance rejection, faster convergence, reduced switching oscillations compared with the baseline SMC, and smooth bounded control inputs suitable for marine actuation systems.

Keywords: *Finite-Time Stability; Integral Sliding Mode; Robust Nonlinear Control; Super-Twisting Algorithm; Unmanned Surface Vehicle*

Symbols

Symbols	Description
$\mathbf{M}$, $\mathbf{C}$, $\mathbf{D}$	parameter matrices of USV
$\mathbf{J}$	Jacobian transformation matrix
$\mathbf{d}(t)$	time-varying disturbances
$\eta = [x \;\; y \;\; \psi]^T$	state vector of USV
$\mathbf{v} = \begin{bmatrix} v_x & v_y & v_\psi \end{bmatrix}^T$	body-fixed velocity vector of the USV
$\mathbf{e}(t)$	trajectory tracking error vector

Abbreviations

USV	unmanned surface vehicle
SMC	sliding mode control
CT-PD	computed-torque proportional-derivative controller
BS-proxy	backstepping-proxy controller
FT-ISSTSMC	finite-time integral super-twisting sliding mode control

1. Introduction

Trajectory tracking for unmanned surface vehicles (USVs) remains difficult due to nonlinear hydrodynamics, uncertain parameters, and environmental forces such as wind, waves, and currents. Recent works have explored reinforcement learning and adaptive dynamic programming for optimal or near-optimal tracking under unknown dynamics [1], [2], [3]. Model predictive control combined with disturbance observers has also been widely studied to address constraints and disturbance rejection [4], [5], [6]. In parallel, robust nonlinear designs based on sliding mode and terminal sliding mode have advanced rapidly, offering finite-time or predefined-time convergence and improved robustness [7], [8], [9]. Event-triggered and quantized-feedback variants further reduce communication and actuator usage while keeping stability guarantees [10], [11].

Fuzzy logic and neural adaptive controllers provide strong approximation capability for uncertain dynamics, including finite-time fuzzy designs and fault-tolerant strategies [12], [13], [14]. Backstepping-based methods remain attractive for strict Lyapunov constructions, including command-filtered and fractional-order observer enhancements [15]. Despite this progress, three gaps remain: (i) many finite-time or predefined-time approaches require conservative knowledge of disturbance bounds; (ii) conventional first-order sliding mode tracking may exhibit chattering or slow convergence under time-varying disturbances; and (iii) learning-based controllers may offer strong performance but typically do not provide explicit finite-time tracking guarantees for the full disturbed model used in realistic marine settings.

Gain-adaptive control has also attracted increasing attention as an effective way to reduce conservative switching gains

Received: 20 April 2026; Revised: 30 September 2026; Accepted: 12 October 2026.

while preserving robustness. For instance, a nonlinear sliding mode controller with two-level gain-learning ability for serial robot manipulators is developed, showing that adaptive gain adjustment can improve tracking performance without excessively large fixed gains [16]. A related high-level adaptive sliding mode strategy was later developed for robotic manipulators with output constraints, where the controller adapts its learning behavior according to the tracking demand [17]. Gain-adaptive robust backstepping has also been investigated for BLDC motor position control, demonstrating that online gain adjustment can improve robustness and reduce unnecessary control effort [18]. These studies motivate the adaptive gain mechanism adopted in this work for USV trajectory tracking under unknown time-varying disturbances.

Motivated by the disturbed three-degree-of-freedom unmanned surface vehicle model used in [19] and the growing interest in higher-order sliding mode designs for marine systems, this paper proposes a robust finite-time integral super-twisting sliding mode controller. The main contributions are threefold. First, an integral sliding variable is developed to reduce steady-state tracking bias caused by persistent environmental disturbances. Second, a super-twisting sliding mode mechanism is embedded to improve robustness while alleviating the chattering commonly observed in first-order sliding mode control. Third, an adaptive gain mechanism is introduced to adjust the switching gains online according to the sliding-variable magnitude, thereby reducing conservative fixed-gain selection while preserving finite-time convergence of the sliding variable and boundedness of the closed-loop signals.

The remainder of this paper is structured as follows: Section 2 presents the preliminaries and formulates the trajectory-tracking problem for the disturbed three-degree-of-freedom unmanned surface vehicle model, including the coordinate transformation and required assumptions. Section 3 develops the proposed finite-time integral super-twisting sliding mode controller, where an integral sliding variable and an adaptive-gain super-twisting law are constructed to enhance disturbance rejection and finite-time convergence of the sliding variable under bounded time-varying disturbances. In Section 4, rigorous stability analysis is provided to establish boundedness of all closed-loop signals and finite-time convergence of the sliding variable, followed by asymptotic convergence of the tracking errors on the sliding manifold. Section 5 reports simulation results and comparative evaluations against benchmark controllers to demonstrate the effectiveness and robustness of the proposed method under time-varying environmental disturbances. Finally, Section 6 concludes the paper and outlines possible directions for future research.

2. Problem formulation

The standard three-degree-of-freedom (3-DOF) planar motion of an unmanned surface vehicle (USV) is illustrated in Fig. 1.

The USV parameters and the inertia, Coriolis–centripetal, and damping matrices are adopted from [19]. The body-fixed frame and the North–East–Down (NED) inertial frame are described in [19].

$$\begin{cases} \mathbf{M}\dot{\mathbf{v}} + \mathbf{C}(\mathbf{v})\mathbf{v} + \mathbf{D}(\mathbf{v})\mathbf{v} + \mathbf{d}(t) = \tau_m \\ \dot{\eta} = \mathbf{J}(\eta)\mathbf{v} \end{cases} \tag{1}$$

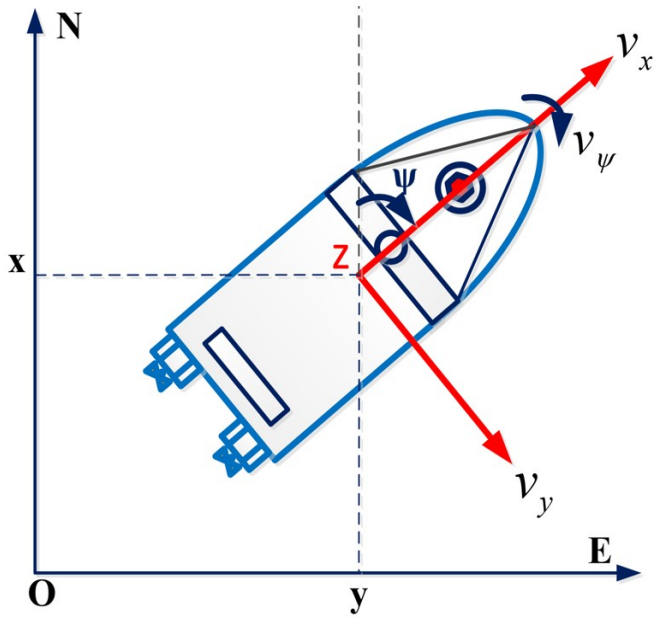


Figure 1: Coordinates of a USV.

where $\eta = [x \;\; y \;\; \psi]^T \in \mathbb{R}^3$ denotes the planar position and yaw angle in the inertial frame; $\mathbf{v} = [v_x \;\; v_y \;\; v_\psi]^T \in \mathbb{R}^3$ denotes the body-fixed velocity vector; $\mathbf{M} \in \mathbb{R}^{3\times3}$ is the inertia matrix; $\mathbf{C}(\mathbf{v}) \in \mathbb{R}^{3\times3}$ is the Coriolis and centripetal matrix; $\mathbf{D}(\mathbf{v}) \in \mathbb{R}^{3\times3}$ is the hydrodynamic damping matrix; $\mathbf{d}(t) \in \mathbb{R}^3$ represents lumped environmental disturbances (wind-wave-current); $\tau_m = [\tau_{mx} \; \tau_{my} \; \tau_{m\psi}]^T \in \mathbb{R}^3$ represents the generalized control force and moment acting on the surge, sway, and yaw channels. In practical implementation, this generalized input can be generated by a low-level thrust-allocation module using multiple thrusters. Therefore, the present work focuses on the high-level trajectory tracking problem in the generalized-force space.

Remark 1. The present study considers the high-level generalized-force control problem. If the physical USV is underactuated and has only surge force and yaw moment, then an additional thrust-allocation or underactuated control layer is required. The extension to strict two-input underactuated actuation is left for future work.

The Jacobian transformation matrix $\mathbf{J}(\eta) \in \mathbb{R}^{3\times3}$ relates the body-fixed frame to the inertial frame and is given by

$$\mathbf{J}(\eta) = \begin{bmatrix} \cos\psi & -\sin\psi & 0 \\ \sin\psi & \cos\psi & 0 \\ 0 & 0 & 1 \end{bmatrix}, \quad \mathbf{J}^{-1}(\eta) = \mathbf{J}^T(\eta) \tag{2}$$

For controller design convenience, the dynamic model (1) is reformulated into a second-order form in η

$$\bar{\mathbf{M}}(\eta)\ddot{\eta} + \bar{\mathbf{C}}(\eta,\dot{\eta})\dot{\eta} + \bar{\mathbf{D}}(\eta,\dot{\eta})\dot{\eta} = \tau_\eta(t) + \tau_{ed}(t) \tag{3}$$

where the transformed matrices and inputs are defined by

$$\begin{aligned} &\bar{\mathbf{M}}(\eta) = \mathbf{J}^{-T}\mathbf{M}\mathbf{J}^{-1}, \bar{\mathbf{C}}(\eta,\dot{\eta}) = \mathbf{J}^{-T}\left(\mathbf{C} - \mathbf{M}\mathbf{J}^{-1}\dot{\mathbf{J}}\right)\mathbf{J}^{-1} \\ &\bar{\mathbf{D}}(\eta,\dot{\eta}) = \mathbf{J}^{-T}\mathbf{D}\mathbf{J}^{-1}, \tau_\eta = \mathbf{J}^{-T}\tau_m, \tau_{ed}(t) = -\mathbf{J}^{-T}\mathbf{d}(t). \end{aligned} \tag{4}$$

The minus sign in $\tau_{ed}(t)$ is absorbed into the lumped disturbance definition; therefore, the boundedness assumption on the disturbance remains unchanged.

Remark 2. Since $\mathbf{J}(\eta) \in \mathbb{R}^{3\times3}$, the inverse satisfies $\mathbf{J}^{-1} = \mathbf{J}^{T}$, which guarantees that (3) is dynamically equivalent to (1) while being written directly in the inertial coordinate η.

Let $\eta_{ref}(t) \in \mathbb{R}^3$ be a smooth desired trajectory (position and yaw) to be tracked. Define the tracking error vector and its derivative as

$$\mathbf{e}(t) = \eta_{ref}(t) - \eta(t), \quad \dot{\mathbf{e}}(t) = \dot{\eta}_{ref}(t) - \dot{\eta}(t) \tag{5}$$

The control goal is to design $\tau_\eta(t)$ such that $\mathbf{e}(t) \to 0$ and $\dot{\mathbf{e}}(t) \to 0$ despite the unknown disturbance $\tau_{ed}(t)$ in (3).

Assumptions:

Assumption 1 (Model regularity and positive definiteness). The inertia matrix $\mathbf{M}$ is symmetric positive definite. The matrices $\mathbf{C}(\mathbf{v})$ and $\mathbf{D}(\mathbf{v})$ are continuous with respect to their arguments. For any compact operating set of the USV motion, there exist positive constants m_1, m_2, c_D, c_C such that

$$\begin{aligned} &m_1\|\mathbf{z}\|^2 \le \mathbf{z}^T\mathbf{M}\mathbf{z} \le m_2\|\mathbf{z}\|^2, \qquad \forall \mathbf{z} \in \mathbb{R}^3, \\ &\|\mathbf{C}(\mathbf{v})\| \le c_C(1+\|\mathbf{v}\|), \\ &\|\mathbf{D}(\mathbf{v})\| \le c_D(1+\|\mathbf{v}\|). \end{aligned} \tag{6}$$

Assumption 2 (Reference regularity). The reference trajectory $\eta ref(t)$, $\dot{\eta} ref(t)$, and $\ddot{\eta}_{ref}(t)$ exist and are bounded for all $t \ge 0$.

Assumption 3 (Bounded disturbance with unknown bound). The transformed environmental disturbance $\tau_{ed}(t) = -\mathbf{J}^{-T}\mathbf{d}(t)$ is bounded, and its time derivative is also bounded,

$$\|\tau_{ed}(t)\| \le \Delta, \qquad \|\dot{\tau}_{ed}(t)\| \le \Delta_1, \qquad \forall t \ge 0, \tag{7}$$

where Δ and Δ_1 are unknown positive constants.

Given the disturbed USV dynamics (3) and the reference trajectory $\eta_{ref}(t)$, design a robust control input $\tau_\eta(t)$ such that:

(1) $\mathbf{e}(t)$ and $\dot{\mathbf{e}}(t)$ converge to zero (or to a small neighborhood if actuator saturation is later considered);

(2) the convergence is achieved despite the unknown disturbance $\tau_{ed}(t)$;

(3) all closed-loop signals remain bounded under Assumptions 1-3.

3. Proposed finite-time integral super-twisting sliding mode controller

This section develops a finite-time integral super-twisting sliding mode control (FT-ISSTSMC) law for the disturbed 3-DOF USV model (3)-(4) and the tracking error definition (5). The reference signals are bounded by Assumption 2, while the closed-loop boundedness of $\eta(t)$ and $\dot{\eta}(t)$ is established in the stability analysis.

3.1 Integral sliding surface design

In [7], a (non-integral) sliding surface of the form $\mathbf{s} = \dot{\mathbf{e}} + \lambda\mathbf{e}$ is adopted for order reduction. To further eliminate steady-state bias caused by persistent disturbances $\tau_{ed}(t)$, we introduce an integral sliding surface. Define an auxiliary integral state $\mathbf{p}(t) \in \mathbb{R}^3$

$$\mathbf{p}(t) = \int_0^t \mathbf{e}(\sigma)\,d\sigma, \quad \dot{\mathbf{p}}(t) = \mathbf{e}(t) \tag{8}$$

Define the integral sliding variable $\mathbf{s}(t) \in \mathbb{R}^3$ as

$$\mathbf{s}(t) = \dot{\mathbf{e}}(t) + \Lambda\mathbf{e}(t) + \Gamma\mathbf{p}(t) \tag{9}$$

where

$$\Lambda = \mathrm{diag}(\lambda_1,\ \lambda_2,\ \lambda_3) > \mathbf{0}, \quad \Gamma = \mathrm{diag}(\gamma_1,\ \gamma_2,\ \gamma_3) > \mathbf{0} \tag{10}$$

Differentiate (9) and use $\dot{\mathbf{p}} = \mathbf{e}$ from (8)

$$\dot{\mathbf{s}} = \ddot{\mathbf{e}} + \Lambda\dot{\mathbf{e}} + \Gamma\mathbf{e} \tag{11}$$

From the tracking error definition (5),

$$\ddot{\mathbf{e}} = \ddot{\eta}_{ref} - \ddot{\eta} \tag{12}$$

From the inertial-coordinate dynamics (3),

$$\ddot{\eta} = \bar{\mathbf{M}}^{-1}(\eta)\left(\tau_\eta + \tau_{ed} - \bar{\mathbf{C}}(\eta,\dot{\eta})\dot{\eta} - \bar{\mathbf{D}}(\eta,\dot{\eta})\dot{\eta}\right) \tag{13}$$

Substitute (13) into (12), then into (11), and multiply both sides by $\bar{\mathbf{M}}(\eta)$ to obtain

$$\begin{aligned} \bar{\mathbf{M}}(\eta)\dot{\mathbf{s}} = \bar{\mathbf{M}}(\eta)\left(\ddot{\eta}_{ref} + \Lambda\dot{\mathbf{e}} + \Gamma\mathbf{e}\right) + \left(\bar{\mathbf{C}} + \bar{\mathbf{D}}\right)\dot{\eta} \\ - \tau_\eta - \tau_{ed} \end{aligned} \tag{14}$$

where $\bar{\mathbf{C}} = \bar{\mathbf{C}}(\eta,\dot{\eta})$ and $\bar{\mathbf{D}} = \bar{\mathbf{D}}(\eta,\dot{\eta})$ for readability.

Now express $\dot{\eta}$ via (5), (8), (9). Since $\dot{\mathbf{e}} = \dot{\eta}_{ref} - \dot{\eta}$, one has $\dot{\eta} = \dot{\eta}_{ref} - \dot{\mathbf{e}}$. Also, from (9), $\dot{\mathbf{e}} = \mathbf{s} - \Lambda\mathbf{e} - \Gamma\mathbf{p}$. Therefore,

$$\begin{aligned} \dot{\eta} &= \dot{\eta}_{ref} - \dot{\mathbf{e}} = \dot{\eta}_{ref} - (\mathbf{s} - \Lambda\mathbf{e} - \Gamma\mathbf{p}) \\ &= \dot{\eta}_{ref} + \Lambda\mathbf{e} + \Gamma\mathbf{p} - \mathbf{s} \end{aligned} \tag{15}$$

Substitute (15) into (14) to isolate the $\mathbf{s}$ term:

$$\begin{aligned} \bar{\mathbf{M}}(\eta)\dot{\mathbf{s}} = &-\left(\bar{\mathbf{C}} + \bar{\mathbf{D}}\right)\mathbf{s} - \tau_\eta \\ &+ \mathbf{f}_I\left(\eta,\dot{\eta},\eta_{ref},\dot{\eta}_{ref},\ddot{\eta}_{ref},\mathbf{e},\mathbf{p}\right) - \tau_{ed} \end{aligned} \tag{16}$$

where the known "lumped" term $\mathbf{f}_I(\cdot)$ is defined consistently as

$$\begin{aligned} \mathbf{f}_I = &\bar{\mathbf{M}}(\eta)\left(\ddot{\eta}_{ref} + \Lambda\dot{\mathbf{e}} + \Gamma\mathbf{e}\right) \\ &+ \left(\bar{\mathbf{C}} + \bar{\mathbf{D}}\right)\left(\dot{\eta}_{ref} + \Lambda\mathbf{e} + \Gamma\mathbf{p}\right) \end{aligned} \tag{17}$$

3.2 Equivalent control structure and reduced sliding dynamics

The transformed input τ_η is selected as

$$\tau_\eta = \mathbf{f}_I - \left(\bar{\mathbf{C}} + \bar{\mathbf{D}}\right)\mathbf{s} - \mathbf{u}, \tag{18}$$

where $\mathbf{u} \in \mathbb{R}^3$ is a robust auxiliary control to be designed.

Substituting (18) into (16) yields the reduced sliding dynamics

$$\bar{\mathbf{M}}(\eta)\dot{\mathbf{s}} = \mathbf{u} - \tau_{ed}. \tag{19}$$

Thus, the controller design becomes the robust stabilization of (19) under the unknown bounded lumped disturbance $\tau_{ed}(t)$.

3.3 Finite-time integral super-twisting robust term

To ensure high robustness while mitigating chattering, we employ a second-order sliding mode (super-twisting) structure and embed it into a finite-time convergence framework. For $\mathbf{x} \in \mathbb{R}^3$, it is defined

- $|\mathbf{x}| = [|x_1| \quad |x_2| \quad |x_3|]^T$,
- $\mathrm{sgn}(\mathbf{x}) = [\mathrm{sgn}(x_1) \quad \mathrm{sgn}(x_2) \quad \mathrm{sgn}(x_3)]^T$,
- $\mathbf{a} \odot \mathbf{b}$ denotes element-wise multiplication.

Introduce an internal super-twisting state $\xi(t) \in \mathbb{R}^3$ governed by

$$\dot{\xi}(t) = -\mathbf{k}_2(t) \odot \operatorname{sgn}(\mathbf{s}(t)), \qquad \xi(0) = \xi_0. \tag{20}$$

The auxiliary robust input is selected as

$$\nu = -\mathbf{k}_1(t) \odot |\mathbf{s}|^{\frac{1}{2}} \odot \operatorname{sgn}(\mathbf{s}) + \xi, \tag{21}$$

where $\mathbf{k}_1(t) = [k_{11}(t)\ \ k_{12}(t)\ \ k_{13}(t)]^T > 0$ and $\mathbf{k}_2(t) = [k_{21}(t)\ k_{22}(t)\ k_{23}(t)]^T > 0$ are adaptive switching gains.

To obtain a standard matched super-twisting structure in the sliding dynamics, choose

$$\mathbf{u} = \bar{\mathbf{M}}(\eta)\nu. \tag{22}$$

Substituting (22) into (19) gives

$$\dot{\mathbf{s}} = \nu - \bar{\mathbf{M}}^{-1}(\eta)\tau_{ed}. \tag{23}$$

Consequently, the final transformed control input can be written as

$$\tau_\eta = \mathbf{f}_I - \left(\bar{\mathbf{C}} + \bar{\mathbf{D}}\right)\mathbf{s} - \bar{\mathbf{M}}(\eta)\,\nu. \tag{24}$$

A key difficulty in sliding mode design is selecting $\mathbf{k}_1, \mathbf{k}_2$ without knowing the disturbance bound. To avoid conservative fixed gains, we propose the following online gain adaptation (component-wise, $i = 1,2,3$):

$$\dot{k}_{1i}(t) = \alpha_{1i}|s_i(t)|^{\frac{1}{2}} - \beta_{1i}k_{1i}(t), \quad k_{1i}(0) > 0 \tag{25}$$

$$\dot{k}_{2i}(t) = \alpha_{2i}|s_i(t)| - \beta_{2i}k_{2i}(t), \quad k_{2i}(0) > 0 \tag{26}$$

where $\alpha_{1i}, \beta_{1i}, \alpha_{2i}, \beta_{2i} > 0$ are design constants.

4. Stability analysis

This section proves the stability of the closed-loop system composed of the disturbed USV dynamics (3), (4), the tracking error definition (5), and the proposed controller (18)–(26).

Before analyzing the closed-loop stability, we first establish the uniform positive definiteness of the transformed inertia matrix. This property is required to guarantee that the transformed inertial dynamics are well posed and that the perturbation term in the sliding dynamics remains bounded.

Lemma 1 (Uniform positive definiteness of $\bar{\mathbf{M}}(\eta)$). Under Assumption 1 and because $\mathbf{J}(\eta)$ is an orthogonal rotation matrix satisfying $\mathbf{J}^{-1}(\eta) = \mathbf{J}^T(\eta)$, the transformed inertia matrix

$$\bar{\mathbf{M}}(\eta) = \mathbf{J}^{-T}(\eta)\mathbf{M}\mathbf{J}^{-1}(\eta) \tag{27}$$

is symmetric positive definite. Therefore, there exist constants $\bar{m}_1, \bar{m}_2 > 0$ such that

$$\bar{m}_1\|\mathbf{y}\|^2 \le \mathbf{y}^T\bar{\mathbf{M}}(\eta)\mathbf{y} \le \bar{m}_2\|\mathbf{y}\|^2, \qquad \forall \mathbf{y} \in \mathbb{R}^3. \tag{28}$$

Proof. From (4), the transformed inertia matrix is given by

$$\bar{\mathbf{M}}(\eta) = \mathbf{J}^{-T}(\eta)\mathbf{M}\mathbf{J}^{-1}(\eta). \tag{29}$$

Since $\mathbf{J}(\eta)$ is an orthogonal rotation matrix, one has

$$\mathbf{J}^{-1}(\eta) = \mathbf{J}^T(\eta), \qquad \mathbf{J}^{-T}(\eta) = \mathbf{J}(\eta). \tag{30}$$

Therefore,

$$\bar{\mathbf{M}}(\eta) = \mathbf{J}(\eta)\mathbf{M}\mathbf{J}^T(\eta). \tag{31}$$

For any $\mathbf{y} \in \mathbb{R}^3$, define $\mathbf{z} = \mathbf{J}^T(\eta)\mathbf{y}$. Since $\mathbf{J}(\eta)$ is orthogonal,

$$\|\mathbf{z}\| = \left\|\mathbf{J}^T(\eta)\mathbf{y}\right\| = \|\mathbf{y}\|. \tag{32}$$

Using Assumption 1, we obtain

$$m_1\|\mathbf{z}\|^2 \le \mathbf{z}^T\mathbf{M}\mathbf{z} \le m_2\|\mathbf{z}\|^2. \tag{33}$$

Because

$$\mathbf{y}^T\bar{\mathbf{M}}(\eta)\mathbf{y} = \mathbf{y}^T\mathbf{J}(\eta)\mathbf{M}\mathbf{J}^T(\eta)\mathbf{y} = \mathbf{z}^T\mathbf{M}\mathbf{z}, \tag{34}$$

it follows from (32)–(34) that

$$m_1\|\mathbf{y}\|^2 \le \mathbf{y}^T\bar{\mathbf{M}}(\eta)\mathbf{y} \le m_2\|\mathbf{y}\|^2. \tag{35}$$

Thus, $\bar{\mathbf{M}}(\eta)$ is uniformly symmetric positive definite for all η. By selecting $\bar{m}_1 = m_1$ and $\bar{m}_2 = m_2$, inequality (28) is obtained. This completes the proof.

The following lemma shows that the proposed leakage-type adaptive laws preserve positivity of the switching gains and prevent unbounded gain growth when the sliding variable is bounded.

Lemma 2 (Positivity and boundedness of adaptive gains). Consider the gain adaptation laws (25) and (26) with initial conditions $k_{1i}(0) > 0$ and $k_{2i}(0) > 0$, where $i = 1,2,3$. If $s_i(t)$ is bounded, i.e., $|s_i(t)| \le \bar{s}_i < \infty$, then the adaptive gains $k_{1i}(t)$ and $k_{2i}(t)$ remain positive and bounded for all $t \ge 0$. In particular,

$$\begin{cases} 0 < k_{1i}(t) \le \max\left\{k_{1i}(0), \frac{\alpha_{1i}}{\beta_{1i}}\bar{s}_i^{\frac{1}{2}}\right\} \\ 0 < k_{2i}(t) \le \max\left\{k_{2i}(0), \frac{\alpha_{2i}}{\beta_{2i}}\bar{s}_i\right\}. \end{cases} \tag{36}$$

Proof. From (25) and (26), one has

$$\begin{cases} \dot{k}_{1i} + \beta_{1i}k_{1i} = \alpha_{1i}|s_i|^{\frac{1}{2}} \ge 0 \\ \dot{k}_{2i} + \beta_{2i}k_{2i} = \alpha_{2i}|s_i| \ge 0. \end{cases} \tag{37}$$

Solving the first equation in (37) gives

$$k_{1i}(t) = e^{-\beta_{1i}t}k_{1i}(0) + \alpha_{1i}\int_0^t e^{-\beta_{1i}(t-\sigma)}|s_i(\sigma)|^{\frac{1}{2}}d\sigma. \tag{38}$$

Since $k_{1i}(0) > 0$ and the integral term in (38) is nonnegative, it follows that

$$k_{1i}(t) > 0, \qquad \forall t \ge 0. \tag{39}$$

Using the boundedness condition $|s_i(t)| \le \bar{s}_i$, we have

$$|s_i(\sigma)|^{\frac{1}{2}} \le \bar{s}_i^{\frac{1}{2}}, \qquad \forall \sigma \ge 0. \tag{40}$$

Substituting (40) into (38) yields

$$k_{1i}(t) \le e^{-\beta_{1i}t}k_{1i}(0) + \alpha_{1i}\bar{s}_i^{\frac{1}{2}}\int_0^t e^{-\beta_{1i}(t-\sigma)}d\sigma. \tag{41}$$

Since

$$\int_0^t e^{-\beta_{1i}(t-\sigma)}d\sigma = \frac{1 - e^{-\beta_{1i}t}}{\beta_{1i}}, \tag{42}$$

we obtain

$$k_{1i}(t) \le e^{-\beta_{1i}t}k_{1i}(0) + \frac{\alpha_{1i}}{\beta_{1i}}\bar{s}_i^{\frac{1}{2}}\left(1 - e^{-\beta_{1i}t}\right). \tag{43}$$

Therefore,

$$0 < k_{1i}(t) \le \max\left\{k_{1i}(0), \frac{\alpha_{1i}}{\beta_{1i}}\bar{s}_i^{\frac{1}{2}}\right\}. \tag{44}$$

Similarly, solving the second equation in (37) gives

$$k_{2i}(t) = e^{-\beta_{2i}t}k_{2i}(0) + \alpha_{2i}\int_0^t e^{-\beta_{2i}(t-\sigma)}|s_i(\sigma)|\,d\sigma. \tag{45}$$

Since $k_{2i}(0) > 0$ and the integral term in (45) is nonnegative, it follows that

$$k_{2i}(t) > 0, \qquad \forall t \ge 0. \tag{46}$$

Using $|s_i(t)| \le \bar{s}_i$, one obtains

$$k_{2i}(t) \le e^{-\beta_{2i}t}k_{2i}(0) + \alpha_{2i}\bar{s}_i\int_0^t e^{-\beta_{2i}(t-\sigma)}d\sigma. \tag{47}$$

Hence,

$$k_{2i}(t) \le e^{-\beta_{2i}t}k_{2i}(0) + \frac{\alpha_{2i}}{\beta_{2i}}\bar{s}_i\left(1 - e^{-\beta_{2i}t}\right). \tag{48}$$

Therefore,

$$0 < k_{2i}(t) \le \max\left\{k_{2i}(0), \frac{\alpha_{2i}}{\beta_{2i}}\bar{s}_i\right\}. \tag{49}$$

Combining (44) and (49) gives (36). Thus, the adaptive gains $k_{1i}(t)$ and $k_{2i}(t)$ remain positive and bounded for all $t \ge 0$. This completes the proof.

Based on Lemmas 1 and 2, the finite-time reachability of the sliding variable is now established using the standard super-twisting structure with a bounded matched perturbation.

Theorem 1 (Finite-time convergence of the sliding variable). Suppose Assumptions 1–3 hold. Consider the USV dynamics (3), the integral sliding surface (9), and the proposed adaptive integral super-twisting sliding mode controller. Let the adaptive gains $k_{1i}(t)$ and $k_{2i}(t)$, $i = 1,2,3$, be generated by (25) and (26) with positive initial values. Assume that, after a finite adaptation transient T_a, the gains become sufficiently large to dominate the bounded matched perturbation

$$\delta(t) = \bar{\mathbf{M}}^{-1}(\eta)\tau_{ed}(t) \tag{50}$$

and its time derivative. Then the sliding variable $\mathbf{s}(t)$ converges to the origin in finite time. Moreover, $\xi(t)$, $\mathbf{k}_1(t)$, and $\mathbf{k}_2(t)$ remain bounded.

Proof. From the reduced sliding dynamics,

$$\bar{\mathbf{M}}(\eta)\dot{\mathbf{s}} = \mathbf{u} - \tau_{ed}. \tag{51}$$

Using $\mathbf{u} = \bar{\mathbf{M}}(\eta)\nu$, one obtains

$$\dot{\mathbf{s}} = \nu - \bar{\mathbf{M}}^{-1}(\eta)\tau_{ed}. \tag{52}$$

Substituting the robust term

$$\nu = -\mathbf{k}_1(t) \odot |\mathbf{s}|^{\frac{1}{2}} \odot \operatorname{sgn}(\mathbf{s}) + \xi \tag{53}$$

into (52) gives

$$\dot{\mathbf{s}} = -\mathbf{k}_1(t) \odot |\mathbf{s}|^{\frac{1}{2}} \odot \operatorname{sgn}(\mathbf{s}) + \xi - \delta(t). \tag{54}$$

The internal super-twisting state satisfies

$$\dot{\xi} = -\mathbf{k}_2(t) \odot \operatorname{sgn}(\mathbf{s}). \tag{55}$$

By Lemma 1, $\bar{\mathbf{M}}(\eta)$ is uniformly positive definite and $\bar{\mathbf{M}}^{-1}(\eta)$ is bounded. By Assumption 3, $\tau_{ed}(t)$ and $\dot{\tau}_{ed}(t)$ are bounded. Hence, on the considered compact operating domain, $\delta(t)$ and $\dot{\delta}(t)$ are bounded. Therefore, there exist positive constants $\bar{\delta}$ and $\bar{\delta}_1$ such that

$$\|\delta(t)\| \le \bar{\delta}, \qquad \|\dot{\delta}(t)\| \le \bar{\delta}_1. \tag{56}$$

For each channel $i = 1,2,3$, (54) and (55) can be written as

$$\dot{s}_i = -k_{1i}(t)|s_i|^{\frac{1}{2}}\operatorname{sgn}(s_i) + \xi_i - \delta_i(t), \tag{57}$$

$$\dot{\xi}_i = -k_{2i}(t)\operatorname{sgn}(s_i). \tag{58}$$

Define

$$z_i(t) = \xi_i(t) - \delta_i(t). \tag{59}$$

Then (57) becomes

$$\dot{s}_i = -k_{1i}(t)|s_i|^{\frac{1}{2}}\operatorname{sgn}(s_i) + z_i(t). \tag{60}$$

Differentiating (59) gives

$$\dot{z}_i = -k_{2i}(t)\operatorname{sgn}(s_i) - \dot{\delta}_i(t). \tag{61}$$

Let

$$\omega_i(t) = -\dot{\delta}_i(t). \tag{62}$$

Then (61) becomes

$$\dot{z}_i = -k_{2i}(t)\operatorname{sgn}(s_i) + \omega_i(t). \tag{63}$$

Since $\dot{\delta}_i(t)$ is bounded, there exists a finite constant $L_i > 0$ such that

$$|\omega_i(t)| \le L_i. \tag{64}$$

Consequently, the pair (s_i, z_i) satisfies the perturbed super-twisting system

$$\dot{s}_i = -k_{1i}(t)|s_i|^{\frac{1}{2}}\operatorname{sgn}(s_i) + z_i, \tag{65}$$

$$\dot{z}_i = -k_{2i}(t)\operatorname{sgn}(s_i) + \omega_i(t), \qquad |\omega_i(t)| \le L_i. \tag{66}$$

According to the standard finite-time convergence condition of the super-twisting algorithm, if there exists a finite time T_a such that, for all $t \ge T_a$,

$$k_{2i}(t) > L_i, \qquad k_{1i}^2(t) > 4k_{2i}(t), \qquad i = 1,2,3, \tag{67}$$

then $s_i(t)$ and $z_i(t)$ converge to zero in finite time. The inequalities in (67) are sufficient gain-dominance conditions. In practice, the design parameters α_{1i}, α_{2i}, β_{1i}, β_{2i}, $k_{1i}(0)$, and $k_{2i}(0)$ are selected such that the adaptive gains can satisfy these conditions after a finite adaptation transient.

Therefore, for each $i = 1,2,3$, there exists a finite time $T_i \ge T_a$ such that

$$s_i(t) = 0, \qquad z_i(t) = 0, \qquad \forall t \ge T_i. \tag{68}$$

Let

$$T_s = \max\{T_1, T_2, T_3\}. \tag{69}$$

Then

$$\mathbf{s}(t) = \mathbf{0}, \qquad \forall t \ge T_s. \tag{70}$$

Thus, the sliding variable converges to the origin in finite time.

It remains to prove boundedness of the internal controller signals. Since $\mathbf{s}(t)$ is finite-time convergent, it is bounded. By Lemma 2, the adaptive gains $\mathbf{k}_1(t)$ and $\mathbf{k}_2(t)$ remain positive and bounded. Moreover, since $z_i(t) = \xi_i(t) - \delta_i(t)$ converges to zero in finite time and $\delta_i(t)$ is bounded, $\xi_i(t)$ is also bounded. Therefore, $\xi(t)$, $\mathbf{k}_1(t)$, and $\mathbf{k}_2(t)$ remain bounded. This completes the proof.

Once the sliding variable reaches the origin, the remaining tracking-error dynamics reduce to a linear exponentially stable integral error system, as shown in the following theorem.

Theorem 2 (Asymptotic convergence of tracking errors). Under Assumptions 1–3 and the controller (20)–(26), if the sliding variable satisfies $\mathbf{s}(t) = \mathbf{0}$ for all $t \geq T_s$, then the tracking error $\mathbf{e}(t)$ and its derivative $\dot{\mathbf{e}}(t)$ satisfy

$$\lim_{t\to\infty} \mathbf{e}(t) = \mathbf{0}, \quad \lim_{t\to\infty} \dot{\mathbf{e}}(t) = \mathbf{0}. \tag{71}$$

Moreover, all closed-loop signals remain bounded on the considered compact operating domain.

Proof. By Theorem 1, there exists a finite time T_s such that $\mathbf{s}(t) = \mathbf{0}$ for all $t \geq T_s$. From (8) and (9), for $t \geq T_s$, one obtains

$$\dot{\mathbf{e}}(t) = -\Lambda\mathbf{e}(t) - \Gamma\mathbf{p}(t), \quad \dot{\mathbf{p}}(t) = \mathbf{e}(t). \tag{72}$$

Define the augmented state

$$\chi(t) = \begin{bmatrix} \mathbf{e}(t) \\ \mathbf{p}(t) \end{bmatrix} \in \mathbb{R}^6. \tag{73}$$

Then (72) becomes

$$\dot{\chi} = \mathbf{A}\chi, \quad \mathbf{A} = \begin{bmatrix} -\Lambda & -\Gamma \\ \mathbf{I} & \mathbf{0} \end{bmatrix}. \tag{74}$$

Since $\Lambda = \mathrm{diag}\{\lambda_1, \lambda_2, \lambda_3\} > 0$ and $\Gamma = \mathrm{diag}\{\gamma_1, \gamma_2, \gamma_3\} > 0$ from (10), each channel of (72) has the characteristic polynomial

$$r^2 + \lambda_i r + \gamma_i = 0, \qquad i = 1, 2, 3. \tag{75}$$

By the Routh–Hurwitz criterion, all roots of (75) have negative real parts. Hence, the matrix $\mathbf{A}$ is Hurwitz. Therefore,

$$\chi(t) \to \mathbf{0}, \qquad \text{as} \qquad t \to \infty. \tag{76}$$

It follows from (73) that

$$\mathbf{e}(t) \to \mathbf{0}, \qquad \mathbf{p}(t) \to \mathbf{0}. \tag{77}$$

Moreover, from (72), one has

$$\dot{\mathbf{e}}(t) = -\Lambda\mathbf{e}(t) - \Gamma\mathbf{p}(t) \to \mathbf{0}. \tag{78}$$

Thus,

$$\lim_{t\to\infty} \mathbf{e}(t) = \mathbf{0}, \quad \lim_{t\to\infty} \dot{\mathbf{e}}(t) = \mathbf{0}. \tag{79}$$

It remains to discuss boundedness of the closed-loop signals. Before T_s, boundedness of $\mathbf{s}(t)$, $\xi(t)$, $\mathbf{k}_1(t)$, and $\mathbf{k}_2(t)$ follows from Theorem 1. Since the closed-loop trajectories are considered on the compact operating domain, and since the reference signals, adaptive gains, and disturbance terms are bounded, the error-related signals $\mathbf{e}(t)$, $\mathbf{p}(t)$, and $\dot{\mathbf{e}}(t)$ remain bounded on the finite interval $[0, T_s]$. For $t \geq T_s$, (72) is an exponentially stable linear system; hence $\mathbf{e}(t)$, $\mathbf{p}(t)$, and $\dot{\mathbf{e}}(t)$ remain bounded and converge to zero.

Furthermore, the reference trajectory and its derivatives are bounded by Assumption 2. On the considered compact operating domain, $\bar{\mathbf{M}}(\eta)$, $\bar{\mathbf{C}}(\eta, \dot{\eta})$, and $\bar{\mathbf{D}}(\eta, \dot{\eta})$ are bounded. Therefore, from the control law (24), the transformed control input τ_η is bounded. Consequently, all closed-loop signals remain bounded. This completes the proof.

5. Simulation results

This section evaluates the tracking performance and robustness of the proposed finite-time integral super-twisting sliding mode controller (FT-ISSTSMC) against three representative benchmark controllers, namely a baseline sliding mode controller (SMC) [20], a computed-torque proportional-derivative controller (CT-PD) [21], and a backstepping-proxy controller (BS-proxy) [22]. All simulations are conducted using the same plant model and time-varying disturbances shown in Fig. 2.

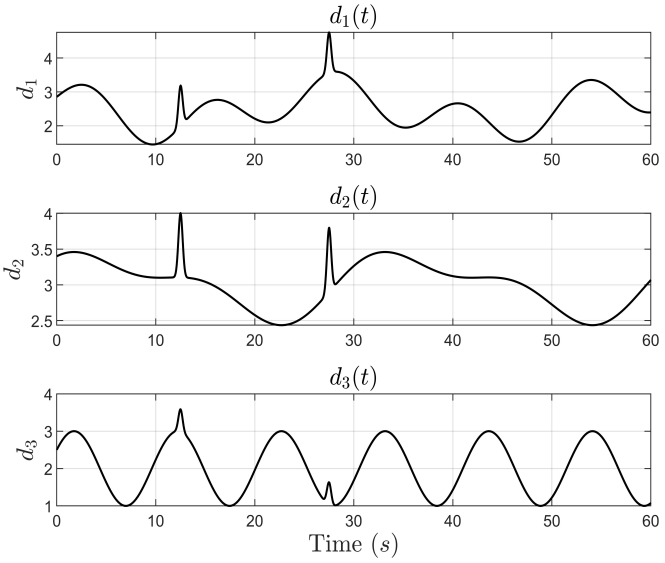


Figure 2: Time-varying disturbances.

The USV parameters and the inertia, Coriolis–centripetal, and damping matrices are adopted from [19]. Controller parameters are used in simulation: $\alpha_1 = [40, 40, 45]^T$, $\alpha_2 = [45, 45, 65]^T$, $\beta_1 = [0.25, 0.25, 0.35]^T$, $\beta_2 = [0.25, 0.25, 0.35]^T$, $k_1(0) = [18, 18, 26]^T$, $k_2(0) = [14, 14, 22]^T$, $\Gamma = \mathrm{diag}\{2, 2, 6\}$, $\Lambda = \mathrm{diag}\{3, 3, 6\}$.

Quantitative performance indices: To provide a quantitative comparison, the following indices are evaluated.

• The root mean square error (RMSE) is defined as

$$\mathrm{RMSE} = \sqrt{\frac{1}{N}\sum_{k=1}^{N} \|e(k)\|^2} \tag{80}$$

• The normalized inverted cosine similarity (NICS) between the reference trajectory and the actual trajectory is defined as

$$\mathrm{NICS} = 1 - \frac{\sum_{k=1}^{N} \eta_{\mathrm{ref}}^T(k)\eta(k)}{\sqrt{\sum_{k=1}^{N} \|\eta_{\mathrm{ref}}(k)\|^2}\sqrt{\sum_{k=1}^{N} \|\eta(k)\|^2}} \tag{81}$$

• The chattering index (CI) of the control input is defined as

$$\mathrm{CI} = \frac{1}{N-1}\sum_{k=1}^{N-1} \frac{\|\tau_m(k+1) - \tau_m(k)\|}{T_s} \tag{82}$$

where T_s is the simulation sampling period.

5.1 Case 1: Circular trajectory tracking under time-varying disturbances

The desired reference trajectory of Case 1 is selected as a circular path in the horizontal plane with a linearly increasing

yaw angle, namely

$$\eta_{\text{ref}}(t) = \begin{bmatrix} x_{\text{ref}}(t) \\ y_{\text{ref}}(t) \\ \psi_{\text{ref}}(t) \end{bmatrix} = \begin{bmatrix} 10\sin(0.2t) \\ -10\cos(0.2t) \\ 0.2t \end{bmatrix}. \tag{83}$$

Figs. 3–8 collectively demonstrate the tracking accuracy, robustness, adaptive behavior, and control smoothness of the proposed FT-ISSTSMC in Case 1. As shown in Figs. 3 and 4, the proposed controller enables the USV to closely follow the desired circular trajectory in the $X-Y$ plane and accurately track $x(t)$, $y(t)$, and $\psi(t)$, with faster convergence, smaller overshoot, and smoother transient responses than the SMC, CT-PD, and BS-proxy controllers. The error responses in Fig. 5 further confirm that the proposed method rapidly suppresses $e_x(t)$, $e_y(t)$, and $e_\psi(t)$ and maintains small steady-state fluctuations despite time-varying disturbances. In Fig. 6, the sliding variables converge quickly to a small neighborhood of zero, supporting the finite-time convergence property established in the theoretical analysis. Fig. 7 shows that the adaptive gains $k_{1i}(t)$ and $k_{2i}(t)$ automatically increase during large-error or strong-disturbance intervals and decrease near the sliding manifold, thereby improving robustness without overly conservative fixed gains. Finally, Fig. 8 indicates that the proposed controller generates bounded and smoother surge, sway, and yaw control inputs with reduced high-frequency oscillations. These results verify that the integral sliding surface, adaptive gain mechanism, and super-twisting structure significantly improve transient tracking, steady-state accuracy, disturbance rejection, and chattering attenuation.

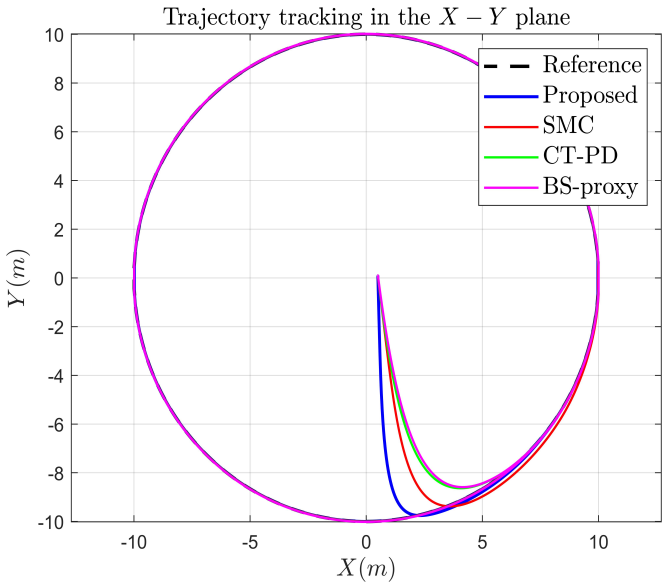


Figure 3: Trajectory in the $X-Y$ plane of Case 1.

5.2 Case 2: Multistep reference validation

To further evaluate the feasibility of the proposed controller beyond smooth circular tracking, an additional multistep reference trajectory is considered. The desired reference trajectory is selected as

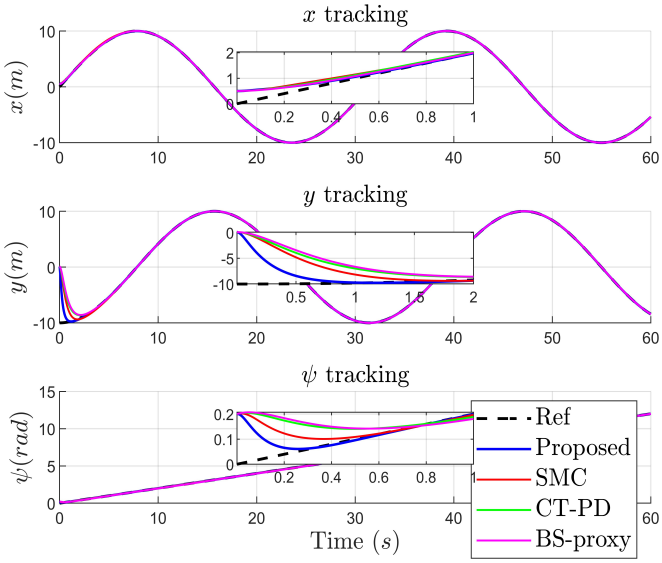


Figure 4: Time responses of $x(t)$, $y(t)$, $\psi(t)$ of Case 1.

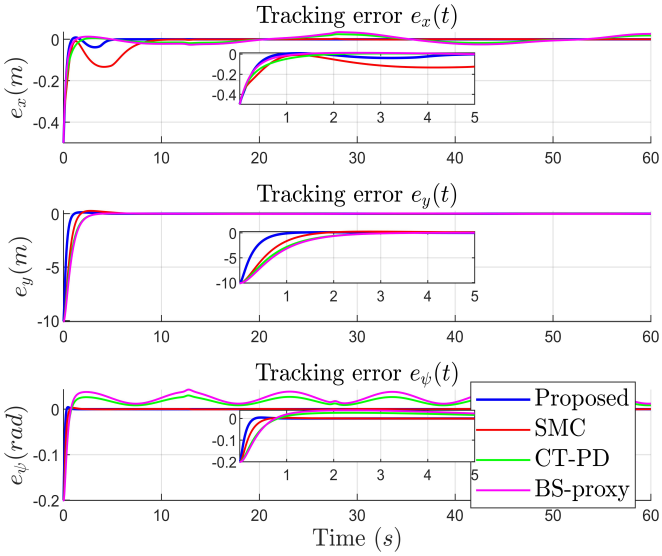


Figure 5: Tracking errors $e_x(t)$, $e_y(t)$, $e_\psi(t)$ of Case 1.

$$\eta_{\text{ref}}(t) = \begin{bmatrix} x_{\text{ref}}(t) \\ y_{\text{ref}}(t) \\ \psi_{\text{ref}}(t) \end{bmatrix} = \begin{cases} \begin{bmatrix} 0 \\ 0 \\ 0 \end{bmatrix}, & 0 \le t < 10, \\ \begin{bmatrix} 4 \\ -3 \\ 0.3 \end{bmatrix}, & 10 \le t < 25, \\ \begin{bmatrix} -3 \\ 5 \\ -0.2 \end{bmatrix}, & 25 \le t < 40, \\ \begin{bmatrix} 2 \\ 1 \\ 0.5 \end{bmatrix}, & 40 \le t \le 60. \end{cases} \tag{84}$$

To avoid discontinuities in the velocity and acceleration commands, the discontinuous multistep signal in (84) is passed through a second-order reference filter before being used in the controller. The filtered reference $\eta_f(t)$ is generated by

$$\ddot{\eta}_f(t) + 2\zeta_f\omega_f\dot{\eta}_f(t) + \omega_f^2\eta f(t) = \omega_f^2\eta ref(t), \tag{85}$$

Table 1: Performance indices of Case 1.

Controller	RMSE	NICS	CI	Settling time (s)
Proposed FT-ISSTSMC	0.5222	0.000921	0.5669	3.4590
SMC	0.8035	0.002182	0.6300	6.6345
CT-PD	0.8884	0.002664	0.5313	58.7830
BS-proxy	0.9352	0.002952	0.5209	> 60

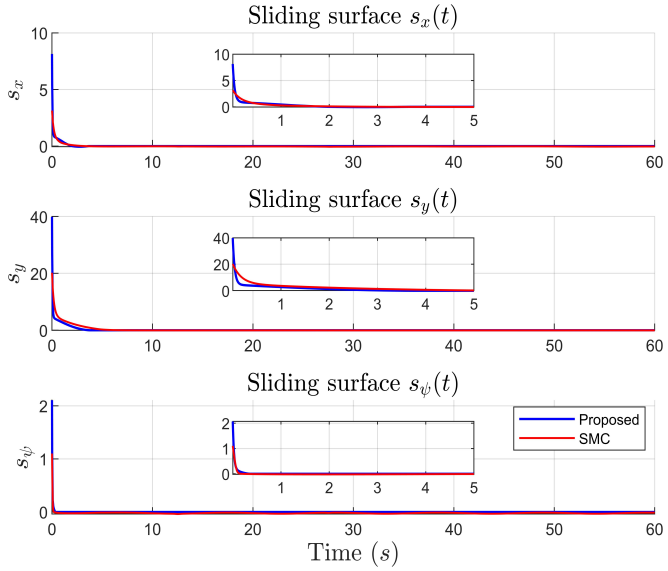


Figure 6: Sliding variables $s_x(t)$, $s_y(t)$, $s_\psi(t)$ of Case 1.

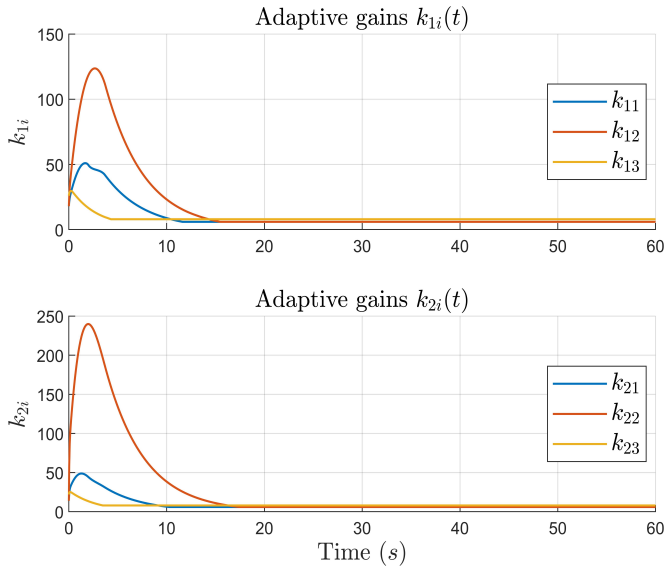


Figure 7: Adaptive gains $k_{1i}(t)$, $k_{2i}(t)$ of Case 1.

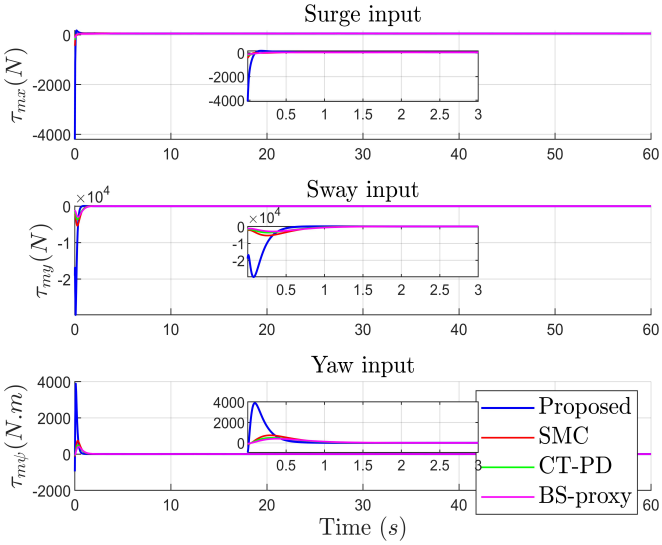


Figure 8: Control inputs $\tau_m(t)$ of Case 1.

where $\omega_f > 0$ and $\zeta_f > 0$ denote the natural frequency and damping ratio of the reference filter, respectively. The signals $\eta_f(t)$, $\dot{\eta}_f(t)$, and $\ddot{\eta}_f(t)$ are then used as the desired reference, velocity, and acceleration in the controller.

Figs. 9–14 present the multistep reference validation of Case 2 using the filtered reference generated by (85), where abrupt changes in the desired position and yaw angle are used to evaluate the transient robustness and practical feasibility of the proposed FT-ISSTSMC. As shown in Figs. 9 and 10, the proposed controller accurately tracks the filtered multistep reference in both the $X-Y$ plane and the time-domain responses of $x(t)$, $y(t)$, and $\psi(t)$, while the benchmark controllers exhibit larger deviations during command transitions. The tracking-error profiles in Fig. 11 further show that the proposed method rapidly suppresses $e_x(t)$, $e_y(t)$, and $e_\psi(t)$ after each reference change and maintains small steady-state fluctuations under time-varying disturbances. Fig. 12 confirms that the sliding variables converge quickly to a small neighborhood of zero, demonstrating the finite-time reaching behavior of the proposed integral super-twisting mechanism. The adaptive gains in Fig. 13 vary automatically according to the transient tracking demand, increasing during large-error intervals and decreasing near the sliding manifold to avoid excessive switching effort. Finally, Fig. 14 shows that the proposed controller generates bounded and comparatively smooth surge, sway, and yaw control inputs during abrupt reference transitions. These results confirm that the proposed FT-ISSTSMC preserves fast convergence, strong disturbance rejection, and reduced switching oscillations compared with the baseline SMC even under nonsmooth multistep command changes.

In summary, the simulation results demonstrate the effectiveness of the proposed FT-ISSTSMC in achieving high-accuracy trajectory tracking for unmanned surface vehicles under dynamic uncertainties and time-varying environmental disturbances. Compared with the benchmark controllers, the proposed method achieves faster convergence, smaller tracking errors, and reduced switching oscillations compared with the baseline SMC while maintaining smooth and bounded control

Table 2: Performance indices of Case 2.

Controller	RMSE	NICS	CI	Settling time (s)
Proposed FT-ISSTSMC	0.0270	0.000025	0.2667	0.5750
SMC	0.0400	0.000054	0.2667	1.0400
CT-PD	0.0532	0.000096	0.2637	58.7850
BS-proxy	0.0615	0.000127	0.2624	> 60

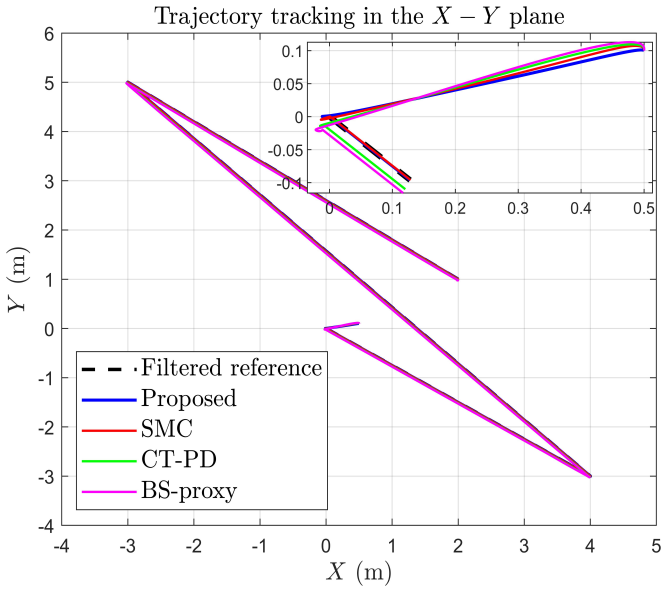


Figure 9: Trajectory in the $X-Y$ plane of Case 2.

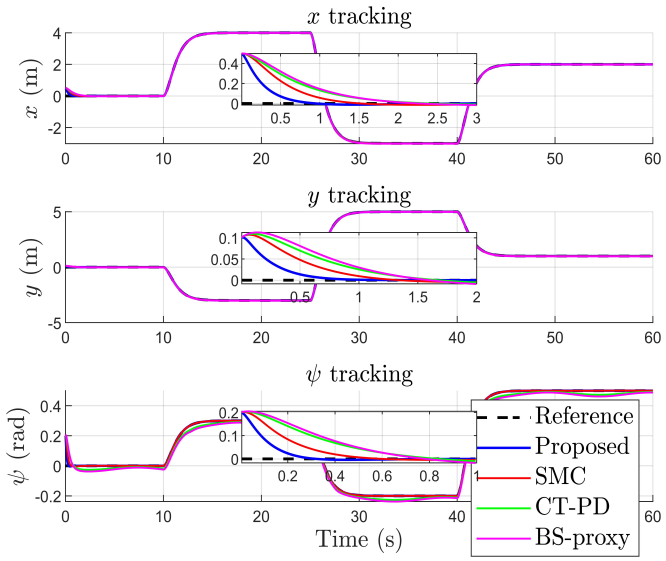


Figure 10: Time responses of $x(t)$, $y(t)$, $\psi(t)$ of Case 2.

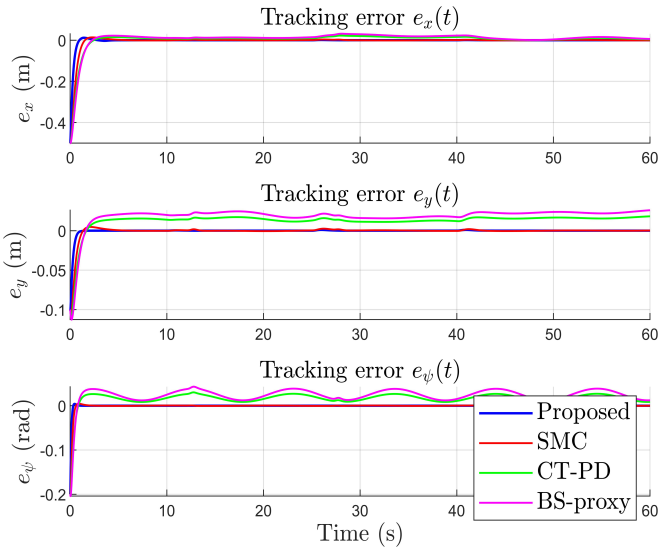


Figure 11: Tracking errors $e_x(t)$, $e_y(t)$, $e_\psi(t)$ of Case 2.

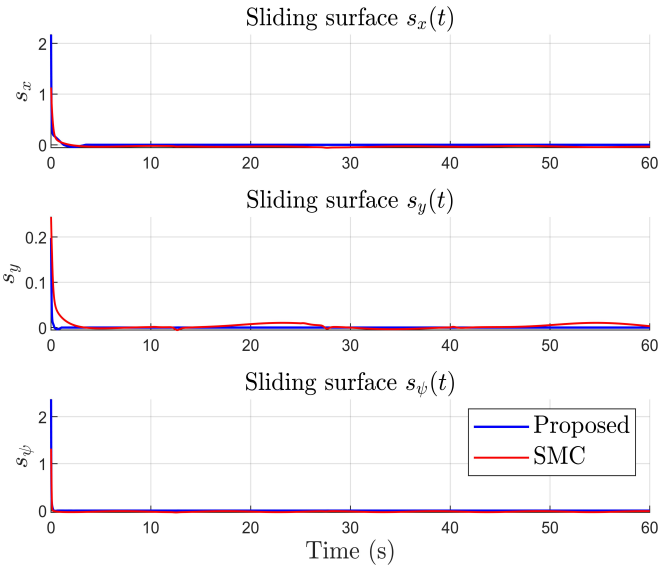


Figure 12: Sliding variables $s_x(t)$, $s_y(t)$, $s_\psi(t)$ of Case 2.

inputs. The finite-time convergence of the sliding variables and the adaptive adjustment of the switching gains further support the theoretical analysis, confirming the robustness and practical applicability of the proposed control scheme in realistic marine environments.

6. Conclusion

This paper proposed an adaptive finite-time integral super-twisting sliding mode controller for trajectory tracking of unmanned surface vehicles subject to nonlinear dynamics and unknown time-varying disturbances. By combining an integral sliding surface, a second-order super-twisting robust term, and adaptive switching gains, the proposed method improves transient tracking accuracy, enhances disturbance rejection,

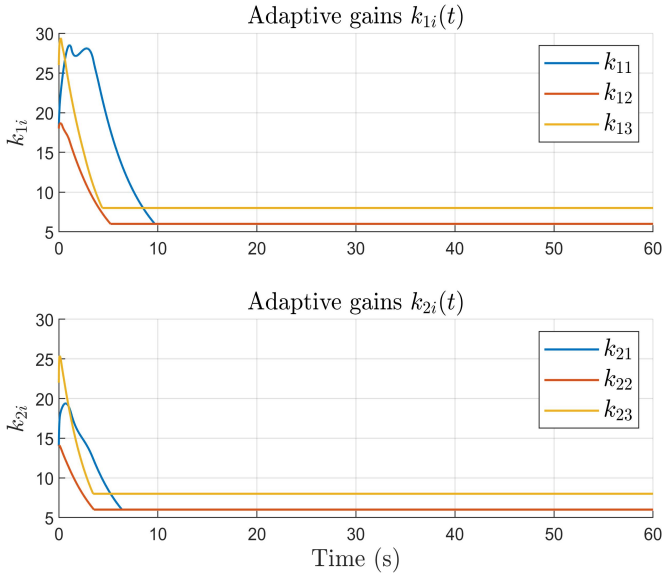


Figure 13: Adaptive gains $k_{1i}(t)$, $k_{2i}(t)$ of Case 2.

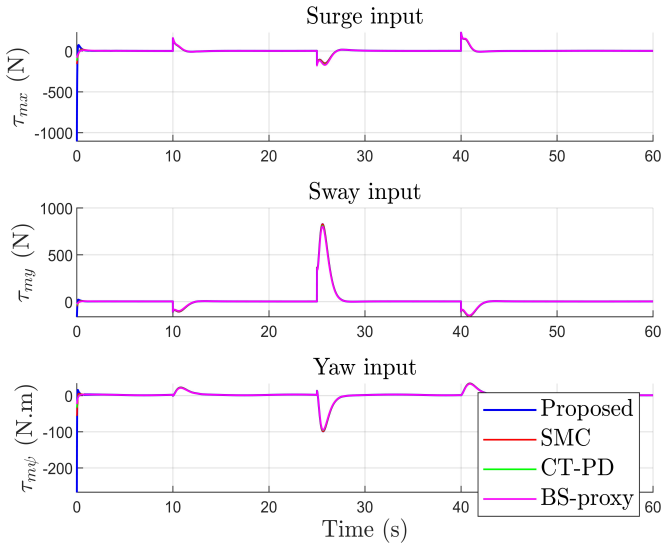


Figure 14: Control inputs $\tau_m(t)$ of Case 2.

and reduces switching oscillations compared with conventional first-order sliding mode control. A stability analysis established finite-time convergence of the sliding variable and asymptotic convergence of the tracking errors on the sliding manifold, while all internal closed-loop signals remain bounded under the stated assumptions. Simulation results for both circular and multistep reference trajectories demonstrated that the proposed controller achieves smaller tracking errors and faster settling time than the SMC, CT-PD, and BS-proxy benchmark controllers. The proposed method also produces smooth and bounded generalized control inputs with competitive chattering indices, confirming its feasibility for high-level generalized-force USV trajectory tracking. Future work will address strict underactuated actuation constraints, actuator saturation, thrust allocation, and experimental validation on a physical USV platform.

References

[1] Y. Liao, Y. Su, and J. Cao, "Trajectory planning and tracking control for underactuated unmanned surface vessels," *Journal of Central South University*, vol. 21, 540–549, 2014, doi: 10.1007/s11771-014-1972-x.

[2] H. Fu, W. Yao, R. Cajo, and S. Zhao, "Trajectory tracking predictive control for unmanned surface vehicles with improved nonlinear disturbance observer," *Journal of Marine Science and Engineering*, vol. 11, no. 10, 2023, ISSN: 2077-1312, doi: 10.3390/jmse11101874.

[3] Y.-H. Chen, S.-Y. Pan, and Y.-Y. Chen, "Trajectory tracking design of autonomous surface vessels with multiple perturbations: A robust adaptive fuzzy approach," *Journal of Marine Science and Engineering*, vol. 13, no. 8, 2025, ISSN: 2077-1312, doi: 10.3390/jmse13081419.

[4] N. Feng, D. Wu, H. Yu, Z. You, and W. Tu, "Disturbance rejection event-triggered robust nonlinear model predictive control for underactuated unmanned surface vehicle against dos attacks without velocity measurements," *ISA Transactions*, vol. 167, pp. 194–205, 2025, ISSN: 0019-0578, doi: 10.1016/j.isatra.2025.08.031.

[5] Y. Hu, B. Li, B. Jiang, J. Han, and C.-Y. Wen, "Disturbance observer-based model predictive control for an unmanned underwater vehicle," *Journal of Marine Science and Engineering*, vol. 12, no. 1, 2024, ISSN: 2077-1312, doi: 10.3390/jmse12010094.

[6] K. Panjavarnam, Z. H. Ismail, C. H. H. Tang, K. Sekiguchi, and G. G. Casas, "Model predictive control for autonomous uav landings: A comprehensive review of strategies, applications and challenges," *The Journal of Engineering*, vol. 2025, no. 1, e70085, 2025, doi: 10.1049/tje2.70085.

[7] N. Wang, C. Qian, J.-C. Sun, and Y.-C. Liu, "Adaptive robust finite-time trajectory tracking control of fully actuated marine surface vehicles," *IEEE Transactions on Control Systems Technology*, vol. 24, no. 4, pp. 1454–1462, 2016, doi: 10.1109/TCST.2015.2496585.

[8] J. Rodriguez, H. Castañeda, A. Gonzalez-Garcia, and J. Gordillo, "Finite-time control for an unmanned surface vehicle based on adaptive sliding mode strategy," *Ocean Engineering*, vol. 254, p. 111 255, 2022, ISSN: 0029-8018, doi: 10.1016/j.oceaneng.2022.111255.

[9] Z. Guo, J. Zhang, Y. Shang, Y. Zhang, L. Zhang, and W. Chen, "Predefined-time global recursive sliding mode control for trajectory tracking of unmanned surface vehicles with disturbances uncertainties," *Ocean Engineering*, vol. 313, p. 119 408, 2024, ISSN: 0029-8018, doi: 10.1016/j.oceaneng.2024.119408.

[10] J. Ning, Y. Ma, T. Li, C. L. P. Chen, and S. Tong, "Event-triggered based trajectory tracking control of under-actuated unmanned surface vehicle with state and input quantization," *IEEE Transactions on Intelligent Vehicles*, vol. 9, no. 2, pp. 3127–3139, 2024, doi: 10.1109/TIV.2023.3339852.

[11] Q. Wang, C. Jiang, J. Ning, L. Hao, and Y. Yin, "Fuzzy course tracking control of unmanned surface vehicle with actuator input quantization and event-triggered mechanism," *Actuators*, vol. 14, no. 3, 2025, ISSN: 2076-0825, doi: 10.3390/act14030130.

[12] W. Wu and S. Tong, "Fixed-time formation fault tolerant control for unmanned surface vehicle systems with intermittent actuator faults," *Ocean Engineering*, vol. 281, p. 114 813, 2023, ISSN: 0029-8018, doi: 10.1016/j.oceaneng.2023.114813.

[13] Y. Bao, J. Gao, and P. Peng, "Fuzzy adaptive fault-tolerant control for an unmanned surface vehicle with prescribed tracking performance," *Frontiers in Robotics and AI*, vol. Volume 12 - 2025, 2025, ISSN: 2296-9144, doi: 10.3389/frobt.2025.1576171.

[14] J. Liu, B. Dai, S. Liu, J. Liu, and T. Li, "Adaptive fuzzy human-in-the-loop control for unmanned surface vehicles in environmental monitoring applications," *Journal of Marine Science and Engineering*, vol. 13, no. 12, 2025, ISSN: 2077-1312, doi: 10.3390/jmse13122270.

[15] B. Liu, Y. Wang, O. Mofid, S. Mobayen, and M. H. Khooban, "Barrier function-based backstepping fractional-order sliding mode control for quad-rotor unmanned aerial vehicle under external disturbances," *IEEE Transactions on Aerospace and Electronic Systems*, vol. 60, no. 1, pp. 716–728, 2024, doi: 10.1109/TAES.2023.3328801.

[16] D. Xuan Ba and J. Bae, "A nonlinear sliding mode controller of serial robot manipulators with two-level gain-learning ability," *IEEE Access*, vol. 8, pp. 189 224–189 235, 2020, doi: 10.1109/ACCESS.2020.3032449.

[17] D. X. Ba, "An intelligent sliding mode controller of robotic manipulators with output constraints and high-level adaptation," *International Journal of Robust and Nonlinear Control*, vol. 32, no. 12, pp. 6888–6912, 2022, doi: 10.1002/rnc.6174.

[18] D. Xuan Ba, H. Yeom, J. Kim, and J. Bae, "Gain-adaptive robust backstepping position control of a bldc motor system," *IEEE/ASME Transactions on Mechatronics*, vol. 23, no. 5, pp. 2470–2481, 2018, doi: 10.1109/TMECH.2018.2864187.

[19] T. T. Tuan, D. H. Vu Quoc, and N. Q. Hung, "Optimal trajectory tracking control for usvs under dynamic uncertainties and time-varying disturbances via pi and irl algorithms," *Journal of Military Science and Technology*, vol. 108, no. 208, 11–20, 2025, doi: 10.54939/1859-1043.j.mst.208.2025.11-20.

[20] V. Utkin, "Variable structure systems with sliding modes," *IEEE Transactions on Automatic Control*, vol. 22, no. 2, pp. 212–222, 1977, doi: 10.1109/TAC.1977.1101446.

[21] M. W. Spong, S. Hutchinson, and M. Vidyasagar, *Robot Modeling and Control*. Hoboken, NJ, USA: Wiley, 2006.

[22] T. I. Fossen, *Handbook of Marine Craft Hydrodynamics and Motion Control*. Chichester, UK: Wiley, 2011.